PERGAMON

Aerosol Science 34 (2003) 1465–1479

Journal of
Aerosol Science

www.elsevier.com/locate/jaerosci

Water adsorption and energetic properties of spark discharge soot: Specific features of hydrophilicity

B.V. Kuznetsov, T.A. Rakhmanova, O.B. Popovicheva*, N.K. Shonija

Moscow State University, Moscow 119 899, Russia

Received 8 May 2002; accepted 16 June 2003

Abstract

Water adsorption was studied for spark discharge soot which is often used as a surrogate for atmospheric soot. Analysis by adsorption gravimetry and calorimetry showed that spark discharge soot exhibits specific features of hydrophilicity. Analysis of the isotherms and heats of water adsorption revealed the peculiarities of the mechanism of surface wetting related to significant changes in the soot microstructure. The first water adsorption/desorption cycle led to irreversible water adsorption and a decrease of the surface area available for water adsorption. Repeated water adsorption/desorption cycles demonstrated swelling phenomena related to the increase of the nitrogen surface area due to interparticle microporosity. The maximum effect of the transformation was observed under exposure to saturated water vapor following the microstructure stabilization. With decreasing temperature the amount of adsorbed water also decreased. Once emitted into the atmosphere the spark discharge soot particles will exhibit irreversible changes in surface area, porosity and hygroscopicity as a result of numerous humidity fluctuations until approaching a stable state of their microstructure due to long exposure to saturated water vapor.

Keywords: Soot; Hygroscopicity; Microstructure

1. Introduction

Emissions from commercial aircrafts have recently gained increasing attention because they comprise a significant fraction of the atmospheric black carbon aerosols, which are suggested to be important components in the cloud–climate interaction and upper tropospheric chemistry (Blake & Kato, 1995). The potential importance of the aircraft-generated soot particles to contrail formation has been recently explored in a series of modelling studies by Karcher, Peter, Biermann, and

* Corresponding author. Tel.: +7-95-939-4954.
E-mail address: polga@mics.msu.su (O.B. Popovicheva).

0021-8502/$ - see front matter © 2003 Elsevier Ltd. All rights reserved.
doi:10.1016/S0021-8502(03)00366-5

Schumann (1996) and Gleitsmann and Zellner (1998). But the ability of the emitted soot particles to be ice nuclei has been left undetermined due to lack of experimental studies of the soot hygroscopic properties under atmospheric conditions. It has been hypothesized that the fresh exhaust soot particles are hydrophobic and would be poor substrates for nucleating water embryos until they have undergone chemical processes through heterogeneous reactions with exhaust gases. But recent studies by Popovitcheva et al. (2000) of the hygroscopicity of the soot particles produced by an aircraft engine combustor have shown their ability for significant water adsorption related to their chemical heterogeneity and microporosity. Moreover, hydration of the soot exhaust particles in the expanding plume and then in the saturated atmosphere may significantly modify the structural and nucleating properties of the soot surface.

At present, different laboratory-made soot types with source-dependent properties are used for atmospherically-relevant studies (Chughtai, Brook, & Smith, 1996). Among those, soot generated by spark discharge between graphite electrodes has recently become subject of intensive studies, especially among researchers interested in the direct generation of airborne material (Kamm, Möhler, Naumann, Saathoff, & Schurath, 1999; Weingartner, Burtscher, & Baltensperger, 1997). This can be attributed to the convenience of operation and high reproducibility of the graphite spark generator, Palas GFG 1000, which produces soot particles without generation of undesirable combustion by-products. In several laboratories Palas soot continues to be used extensively to study the heterogeneous chemistry of reactive gases (Kamm et al., 1999; Kalberer, Ammann, Gäggeler, & Baltensperger, 1999b) and the role of adsorbed water in reactivity (Kalberer, Ammann, Arens, Gaggeler, & Baltensperger, 1999a). Determination of Palas soot hygroscopicity and its ability to act as condensation nuclei (Kotzick, Panne, & Niessner, 1997; Nink, Saatholf, Schnaiter, & Mohler, 2001) requires knowledge on water adsorptivity over a wide range of atmospheric conditions. Unfortunately such studies have been rare until now.

The bulk mechanical properties of particulate solids are often strongly influenced by the interaction with condensed vapors. The influence of moisture on the stability of the particle agglomerates has received considerable attention (Coughlin, Elbirli, & Vergara-Edwadrs, 1982). Hydration of Palas soot particles in the humid atmosphere leading to changes in the structure of the particles has been observed by Weingartner et al. (1997) and Mikhailov, Vlasenko, Kiselev, and Ryshkevich (1998). Shrinkage by nearly 10% of the soot agglomerates becomes noticeable already at the relative humidity RH $\cong$ 70%. It has been proposed that soot agglomerates collapse to a more compact structure under the influence of capillary forces exerted by water condensed in the interstitial space of contacting particles.

Water molecules may penetrate the micropores of the porous adsorbents, thereby increasing the surface area. This swelling effect has been observed for combustor soot by Popovitcheva et al. (2000). Previously collected data (Bailey, Cadenhead, Davies, Everett, & Miles, 1971; Gregg & Sing, 1982) have provided substantial support for the fact that the low-pressure hysteresis observed for these systems is associated with the intercalation of the adsorbate molecules in the narrow pore spaces leading to irreversible changes in the pore structure. It has also been shown that structure deformation of the swelling carbonaceous fibers is accompanied by an endothermic effect (Poloiakova, Tarasevich, & Poloiakov, 1994).

This study has been undertaken to investigate the adsorption and energy properties of spark discharge soot and specific features of its hydrophilicity. The results of this study led to a better understanding of the mechanism of the soot surface wetting and the dependence of the surface

wetting on temperature. It has been possible to investigate structural changes and swelling effects systematically, using the classical method of repeated adsorption/desorption cycles to study the isotherm reversibility and microstructure changing. We will first illustrate the hygroscopicity of spark discharge soot in comparison with reference hydrophobic and hydrophilic substrates as well as with aircraft combustor soot.

2. Experimental

Palas soot was produced in pure argon (99.9999%, Messer Griesheim) by means of a graphite spark generator (GfG 1000, Palas) as it was done by Kamm et al. (1999). The soot was collected on a teflon support. Due to the high inertness of the teflon material we believe that there is no influence of the sampling procedure on soot chemistry itself. The total mass of the soot sample was equal to 70.7 mg. The specific surface area, S, was determined by thermodesorption spectrometry, typically used for the measurement of surface areas from 0.1 up 500 m^2/g of different adsorbents with a precision of 5–10% (Kiselev & Jasin, 1985). The intensities of the thermodesorption spectra of the low-temperature N_2 adsorption were compared for both a reference sample (having a known surface area) and Palas soot. A reference sample (chanel soot) with a chemical nature similar to that of the studied sample was chosen. The specific area of the reference sample was determined previously by the BET method (Gregg & Sing, 1982). In our study, comparison with a reference soot of $S = 80\ m^2/g$ provided us with an estimate of the specific surface area of Palas soot.

The first series of experiments consisted of three measurements of the adsorption/desorption cycles of water isotherms on the same soot sample at a temperature of 303 K. It was performed using a volumetric technique which is a conventional method for the measurement of adsorption isotherms allowing to determine the equilibrium pressure after adsorption in the calibrated volumes with an accuracy of 1–3% (Brunauer, 1945). Before adsorption, the soot sample was treated to remove the pre-adsorbed water and impurities which may have been accumulated on the soot surface from ambient atmosphere. The soot sample was heated at 473 K and outgassed at 10^{-3} Torr for approximately 30 h. The final criterion to finish the treatment was the absence of desorption from the soot surface during 30 min under vacuum. This procedure reduced the soot mass by about 1%.

The pre-treatment of the soot sample is absolutely necessary to ensure the reproducibility of experimental results by removing surface impurities. The conditions of the sample pre-treatment were chosen to prevent any changes in either the structure or chemical nature of the surface itself (Kiselev & Kovaleva, 1959; Kiselev, Kovaleva, & Korolev, 1961). Thus, surface area and porosity of the soot sample remained the same, as well as the surface composition. The same procedure was repeated after each adsorption/desorption.

Simultaneously with the measurement of the adsorption isotherms, the differential heat of the water adsorption was also obtained, using a calorimeter of the Calvet type (Calvet & Prat, 1958) coupled with the volumetric setup, as described in detail in Derkaui, Kiselev, and Kuznetsov (1985).

The series of the next fourth to sixth measurements of the adsorption/desorption cycles for the water isotherms was done at $T = 279$, 292 and 303 K, respectively, using a gravimetric technique employing electromagnetic scales (Brunauer, 1945). In the gravimetric method the adsorption equilibrium was reached after the mass changing ceased. Depending on pressure, it took from 2 to 10 h to reach equilibrium. The treatment of the soot sample before each new cycle was similar to

that in the volumetric setup, i.e., until the sample weight reached a constant value. The sensitivity of the electromagnetic scales was 0.1 mg/g, and the overall experimental error of the gravimetric method amounted to 1–3%. After reaching the saturation pressure in the fourth cycle at $T = 279$ K, the soot sample was exposed to saturated water vapor for 120 h. Then fifth and sixth cycles of the water adsorption were measured.

The isotherm of N_2 adsorption was measured at $T = 77$ K after the sixth cycle to observe a possible change in the surface area. The specific surface area of the soot was determined once more by applying the BET theory to the N_2 adsorption data taking into account the buoyancy correction (Kuznetsov, Moreva, & Rakhmanova, 2000). The seventh and last water adsorption/desorption cycle was done at 291 K to observe the isotherm reversibility at the end of the adsorption measurements. Finally, the heats of the soot immersion in water and benzene were measured in a calorimeter with constant heat exchange (Isirikyan, Kiselev, & Muttick, 1957).

3. Results and discussion

3.1. Adsorption and energy characteristics of Palas soot

The specific surface area of Palas soot has been determined to 308 ± 30 m^2/g by the thermodesorption comparative analysis, which is in agreement with the value of 300 m^2/g reported by Kalberer et al. (1999a,b). The marked difference of our result from the value of 395 m^2/g obtained by Helsper et al. (1993) is most likely due to different operation conditions during the soot generation, as discussed by Schwyn, Garwin, and Schmidt-Ott (1988). This idea is supported by the fact that Palas soot produced during the AIDA campaign exhibited a primary particle diameter of 6.6 ± 1.7 nm (Wentzel, Gorzawski, Naumann, Saathoff, & Weindruch, 2003) in contrast to the value of 5 nm reported by Helsper et al. (1993).

The peculiar nature of the water adsorption on carbonaceous adsorbents is related to a relatively low dispersion energy between water molecules and graphite sheets which leads to a strong dependence on the presence of hydrophilic sites, so called primary adsorption centers (Dubinin, 1980). According to the fundamental mechanism of the water adsorption on carbonaceous adsorbents the initial water adsorption is likely to be due to the oxygen containing groups which may act as the primary adsorption sites. Graphitized soot Graphon possesses a well-defined hydrophobic and nearly homogeneous surface with a very small fraction of hydrophilic heterogeneities (Young, Chessick, Healey, & Zettlemoyer, 1954). This is why the typical isotherm of water adsorption on hydrophobic Graphon is concave and the small increase in adsorption is observed only at high relative pressures due to the secondary mechanism of adsorption on previously adsorbed water molecules (Type III of BDDT classification (Gregg & Sing, 1982)).

The adsorption isotherm on spark discharge soot for the first adsorption/desorption cycle at $T = 303$ K is shown in Fig. 1a. This adsorption isotherm cannot be attributed to the Type III adsorption mechanism because it exhibits a convex shape at the lowest relative pressures, probably due to the existence of a significant amount of primary adsorption centers on the surface. Oxygen containing groups on the surface of Palas soot have been observed by Kirchner, Scheer, and Vogt (2000) using FTIR spectroscopy. They are attributed to the surface functionalities, such as a –C–O, aromatic –C═O and carboxylic C═O groups. Their existence can possibly be due to impurities in

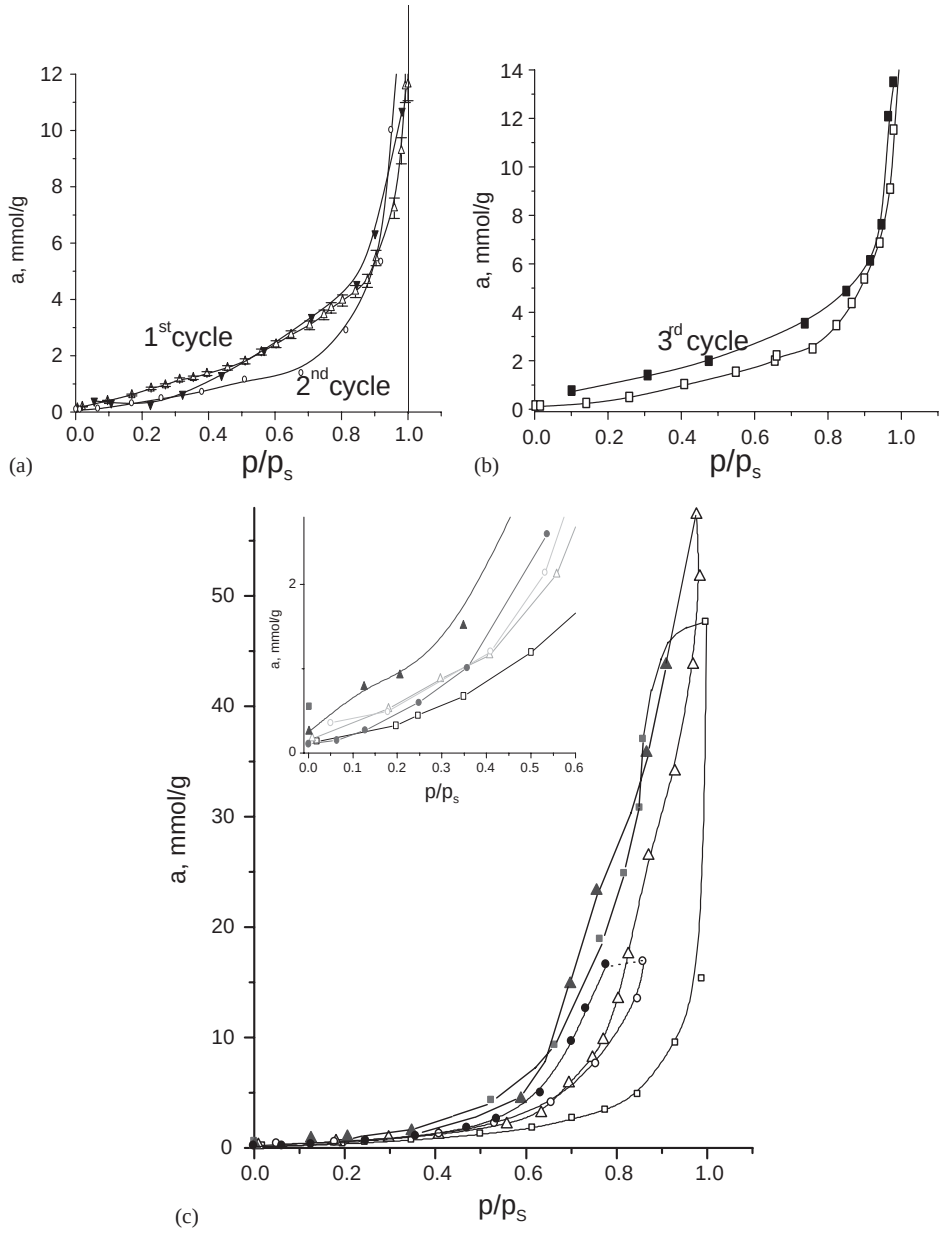

Fig. 1. Isotherms of water adsorption (open) and desorption (closed symbols) on Palas soot: (a) at 303 K, triangles—first cycle, circles—second, (b) squares—third cycle, (c) squares—fourth cycle at 279 K, triangles—fifth cycle at 291 K, circles—sixth cycle at 303 K. Inset: low pressure part of isotherms. Error bars are shown for first cycle.

the graphite rod (Kirchner et al., 2000) and/or the argon supply system (Kalberer et al., 1999a,b). The amount of water corresponding to one monolayer, a_m, may be determined by applying the BET theory to the water adsorption data. Assuming that one water molecule is adsorbed on each primary

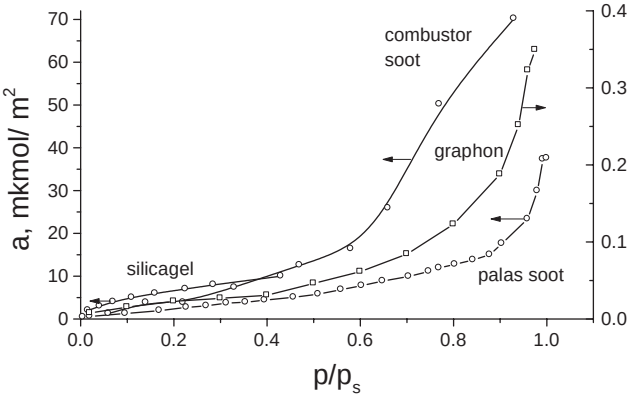

Fig. 2. Absolute isotherms of water adsorption on Palas soot at 303 K, combustor soot, and silica gel, and Graphon multiplied in 50 times.

site in the range of low relative pressures up to 0.1, we can estimate the amount of primary adsorption sites to $a_m \cong 0.54$ mmol/g. Then the part of the surface area of Palas soot available for water adsorption is obtained to be equal to $S_{H20} \cong 33 \pm 1$ m^2/g assuming a cross-sectional area of water molecules of 0.1 nm^2 (Gregg & Sing, 1982). This result indicates that one-tenth of the total surface of Palas soot is hydrophilic and the remainder is hydrophobic.

Fig. 2 plots the absolute adsorption isotherms calculated for unit surface for Palas soot. For comparison, the absolute adsorption isotherms for Graphon, taken from (Young et al., 1954), are also plotted. Values for the specific surface areas of 310 and 83 m^2/g were used for Palas soot and for Graphon (Young et al., 1954), respectively. For comparison the amount of water adsorbed on Graphon at BETa_m amounts to only about $\frac{1}{1500}$ of the value that would be expected in the case of closest molecular packing on the solid surface (Young et al., 1954).

The analysis of the adsorption/desorption isotherms in the first cycle gives useful information about the Palas soot porosity. In Fig. 1a one can see a narrow high-pressure hysteresis in the adsorption and desorption parts of the first cycle that is a well-established characteristic of adsorbents with mesopores of radius larger then 2 nm (Bailey et al., 1971). The slope of the hysteresis is related to the form of the pore size distribution. The onset of the hysteresis loop at $p/p_s \cong 0.6$ indicates capillary condensation in the mesopores of minimum radius which is estimated to be equal to $\geqslant 2.1$ nm using the Kelvin–Thomson equation (Gregg & Sing, 1982).

The location of mesopores in the soot structure can be determined from electron microscopy analysis. It was observed that Palas soot consists of agglomerates with primary particle diameters between 5 and 10 nm (Weingartner et al., 1997; Helsper et al., 1993; Wentzel et al., 2003). The internal microstructure of the primary particles appears (Wentzel et al., 2003) to be totally amorphous without any distinctive micropores. This is different from the onion-like microstructure of combustor soot particles which determines their internal microporosity (Popovitcheva et al., 2000). Therefore, it is reasonable to conclude that the primary porosity of Palas soot is determined by mesopores to be identified with cavities between the primary particles.

The desorption branch of the first cycle is located below the adsorption one at the relative pressure of $p/p_s < 0.5$, see Fig. 1a. This seems to be related to a decrease of the surface area available for

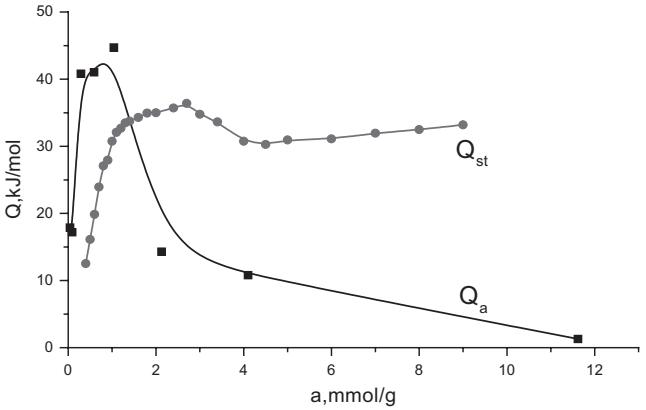

Fig. 3. Differential and isosteric heats of water adsorption on Palas soot.

water adsorption during the adsorption/desorption process. It can be attributed to the change in the soot structure due to capillary forces, leading to a shrinking of the agglomerates and an increase of the fractal dimension as observed by Mikhailov et al. (1998) and Weingartner et al. (1997). As a result of this structure transformation, a significant amount of water molecules, approximately 0.5 mmol/g, is remaining in the small internal cavities, leading to the irreversible adsorption observed in the first cycle, see Fig. 1a.

The second adsorption cycle shown in Fig. 1a also leads to a decrease of the amount of adsorbed water probably due to the continuing structure transformation. The water-accessible surface area amounts to about $16 \pm 0.5\ m^2/g$.

The specific behavior of the heat of adsorption on Palas soot may serve as the confirmation for the suggested mechanism of the structure transformation during the water adsorption. Fig. 3 shows the dependence of the differential heat of water adsorption, Q_a, on the amount of adsorbed water at 303 K measured in the second adsorption cycle. At small relative pressures the differential heat of water adsorption is $Q_a \cong 17$ kJ/mol, close to the energy of hydrogen bonding between the primary adsorption centers and water molecules. The increase of the differential heat of adsorption up to 44 kJ/mol accompanies the water cluster formation on the primarily adsorbed water molecules. This is why the differential heat of adsorption exhibits a value close to the heat of water condensation, $L \cong 43.8$ kJ/mol. With further increase in the relative pressure, Q_a should approach the heat of water condensation when the complete surface coverage by water molecules has been established. But in our experiments Q_a approaches a maximum value of $Q_a^{max} \cong 44$ kJ/mol at $a \cong 1$ mmol/g and then it drops.

It is possible to suggest that the resulting capillary forces acting between the particles cause the morphological changes (Coughlin et al., 1982). It is seems that the endothermic effect $\Delta Q \geqslant 40$ kJ/mol accompanies the structure transformation of Palas soot at $p/p_S > 0.6$ since the measured heat of adsorption is decreasing down to low values. A similar effect was observed by Poloiakova et al. (1994) for the swelling of carbonaceous fibers. It is interesting to note also that the decrease of Q_a takes place at $p/p_s > 0.6$ where a significant shrinkage of the Palas soot agglomerates (more 10%) was observed by Weingartner et al. (1997).

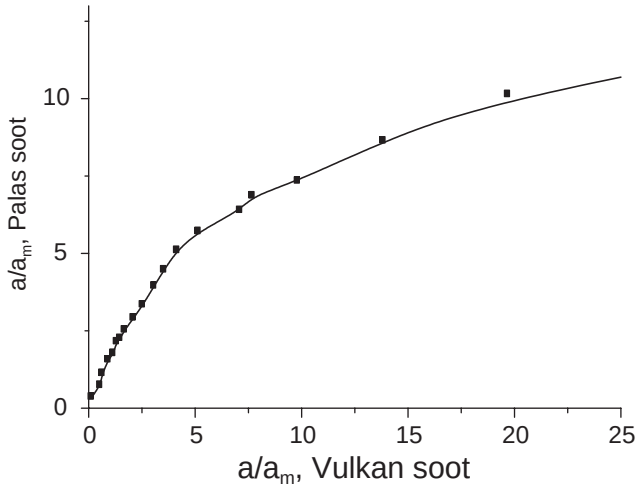

Fig. 4. Comparative plot of water adsorption on Palas soot at 303 K (first cycle) using the adsorption data on graphitized soot Vulkan 7H.

To clarify the peculiarities of the adsorption mechanism on Palas soot it is useful to carry out a comparative analysis (Karnaukhov, Fenelov, & Gavrilov, 1989) using the standard adsorption isotherm determined for the nonporous surface of graphitized soot as a reference sample. For this purpose, we plotted the dimensionless adsorption, a/a_m, for the material under consideration against the values determined for a reference sample (Vartapetian & Voloshchuk, 1995). The similarity of the mechanism of the water adsorption on the primary centers at low pressures for all soot types is clearly demonstrated in the linear region of the graph at the initial range of a/a_m. Fig. 4 presents the comparative graph for Palas soot. The water adsorption isotherm for graphitized soot Vulkan 7H was chosen as a standard isotherm (Vartapetian & Voloshchuk, 1995). The value of a_m for Vulkan 7H soot was obtained to 0.0065 mmol/g applying the BET theory. The resulting graph consists of two parts. The initially linear part up to $a/a_m \cong 2.5$ indicates the creation of independent water clusters from two to three water molecules near the primary adsorption sites. For relative pressures above $p/p_S \cong 0.6$ the experimental points deviate downwards from a straight line indicating the confluence of the water clusters.

The third adsorption/desorption cycle reveals new features of the structure transformation phenomenon. Analysis of the adsorption/desorption isotherm shown in Fig. 1b indicates that the water surface area is similar to that of the second cycle, about 16 ± 0.5 m^2/g. But the desorption branch of the third cycle exhibits a wide low-pressure hysteresis if compared with the first cycle isotherm. This may be associated with the swelling process observed in microporous fibers, clays, zeolites, and carbons (Bailey et al., 1971). This fact shows that the structure changes in the first and second cycles lead to the irreversible morphological transformation clearly observed in the third cycle. Probably it is associated with the creation of microporosity in the soot particles.

If the structural deformation exceeds the elastic limit of the medium, defects and cracks may appear in the places of the lowest energy. The drop in the heat of adsorption observed in Fig. 3 may be ascribed to the work needed for the breaking of C–C bonds and deformation of the agglomerate structure (Stoeckli, Perret, & Mena, 1980). Defects and cracks are the places for micropore opening.

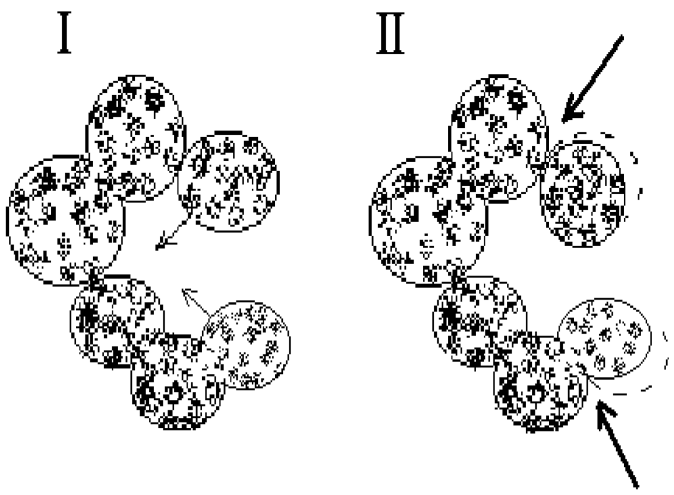

Fig. 5. Schematic representation of possible restructuring of Palas soot agglomerates. (I)—soot agglomerate under water exposure. Arrows indicates the direction of the displacement of the exterior particles. (II)—soot agglomerate after restructuring. Dashed lines show the place of the exterior particles before restructuring. Arrows indicates the places of the opening microporosity in the cavities between particles.

Fig. 5 presents a qualitative scheme of the transformation process with shrinkage of the agglomerates as the first step and the creation of micropores, most likely in the regions around points of contacts of the soot globules, as a result. The appearance of the new micropores is probably accompanied by the formation of a new hydrophobic surface, identified as a decrease of the surface area accessible for water molecules in each subsequent adsorption cycle.

It is reasonable to suggest that the strongest influence of water adsorption on the soot microstructure should arise under exposure to saturated vapor when the deformation of the pore structure by adsorption forces exceeds the elastic limit of the porous medium. To confirm this statement the soot sample was exposed to saturated vapor for 120 h after approaching a relative humidity $\cong$ 100% in the fourth cycle. The resulting data for the fourth adsorption/desorption cycle are shown in Fig. 1c. Intensive water condensation in the soot meso and macropores took place leading to a significant increase of the amount of adsorbed water up to 40 mmol/g at high relative pressures. A significant hysteresis loop was also observed. The consequences of the structural modification exerted by saturated vapor exposure will be discussed below.

3.2. Temperature effect

For the majority of adsorbents and adsorbates the amount of adsorbed material increases with decreasing temperature (Brunauer, 1945). However, an "unusual" reversible order of the water isotherms was observed for the graphitized soot Graphon (Zettlemoyer & McCafferty, 1973) as well as for combustor soot (Popovitcheva, Trukhin, Persiantseva, & Shonija, 2001). Such unusual dependence of the adsorption on temperature can be related to the hydrophobic nature of the surface. It may be explained by the small value of the isosteric heat of adsorption, Q_{st}, in comparison with the heat of water condensation, L (Zettlemoyer & McCafferty, 1973). A similar reason was also indicated for the system graphitized soot—NH_3 (Bomchil, Harris, Leslie, Tabony, & White, 1979).

To study the temperature effect on adsorption we have measured the following series, from the fourth to the sixth cycles, at 279, 291 and 303 K, respectively. Fig. 1c shows the adsorption/desorption isotherms for the fourth and the fifth cycles which decrease with temperature. The value of the isosteric heat of adsorption Q_{st} was calculated as

$$Q_{st} = RT^2 \left.\frac{\mathrm{d}\ln p}{\mathrm{d}T}\right|_a$$

at a given amount a of adsorbed water (Gregg & Sing, 1982). The Q_{st} values calculated using the adsorption data at 279 and 291 K are plotted in Fig. 3. The value of the isosteric heat of adsorption is less than the heat of water condensation, over the complete range of a. This specific feature was also demonstrated for graphitized hydrophobic soot by Vartapetian, Voloshchuk, Isirikyan, and Poliakov (1993). The isotherm in the sixth cycle is similar to that in the fifth cycle (see Fig. 1c).

Analyzing the fourth to sixth adsorption/desorption cycles, the second important finding was the existence of a wide low-pressure hysteresis which may be associated with a swelling process of the microporous adsorbents (Bailey et al., 1971). This confirms the creation of micropores after the first series of the adsorption measurements. Based on these experiments, we concluded that microporosity created in Palas soot is the result of the many times repeated adsorption/desorption cycles and exposure to saturated vapors.

To confirm this suggestion the isotherm of the nitrogen adsorption was measured after the sixth cycle. The specific surface area, S_{N2} of Palas soot, was determined to be 640 m^2/g, applying the BET theory. This value is two times larger than the one obtained by the thermodesorption analysis of fresh Palas soot. This increase may be related to the formation of a new surface in the open micropores. To check this assumption we examined the structural properties of Palas soot using the N_2 adsorption data.

The isotherm of the N_2 adsorption is classified as Type I and its mechanism is typically discussed in terms of Dubinin's theory of pore filling (Gregg & Sing, 1982). The micropore volume and the average pore size can be determined by means of the fundamental Dubinin–Astakhov equation (Dubinin & Stoeckli, 1980)

$$a = \frac{W_0}{v^*} \exp(-(A/\beta E_0)^2), \tag{6}$$

where a represents the amount adsorbed at a relative pressure p/p_S; W_0 is the limiting volume of adsorption or the volume of the micropores, and v^* is the molar volume of the adsorbates; A is the change in Gibbs free energy upon adsorption, defined by

$$A = RT \ln(p_S/p) \tag{7}$$

and E_0 is the characteristic energy of adsorption; β is the affinity coefficient of the characteristic curves. For nitrogen $\beta = 0.37$ and $v^* = 34.7$ cm^3/mol (Dubinin, 1965).

In the plausible model for a half width x of the slit-shaped micropores there exists an approximate relationship between x and the characteristic energy in the form $x = k/E_0$

$$k = (13.028 - 1.53 \times 10^{-5} E_o^{3.5}) \text{ kJ nm/mol}.$$

Using this equation we estimated the half-width of the micropores to be about 1 nm, a reasonable value for micropores which may have formed after the transformation in the original contact

areas of the primary particles as sketched in Fig. 5. Now it is easy to calculate the total geometric surface area of the micropores as $S = W_0/2x$. The value obtained is $\cong 270\ m^2/g$ which determines the difference between the surface area for fresh Palas soot and that after its exposure to saturated vapors ($\cong 640\ m^2/g$).

The third conclusion may be inferred from the seventh (the last) adsorption/ desorption cycle. It was repeated at 291 K especially to be compared with the adsorption data in the fifth cycle. It was found that the adsorption and desorption parts of the seventh cycle coincided well with those of the fifth cycle. It seems that after the numerous humidity fluctuations and the long exposure to saturated vapor the *stabilization* of the soot microstructure after the fifth cycle finally occurred. Also hygroscopicity has reached its stable value: in the fourth cycle the water accessible surface area amounted to $19 \pm 1\ m^2/g$, while in the sixth cycle $S_{H2O} \approx 30 \pm 1.5\ m^2/g$, similar to that obtained in the fifth cycle.

3.3. Comparative hydrophilicity analysis

The data presented above allow us to analyze the hydrophilicity of Palas soot. We will classify the extent of hydrophilicity using two ways: (1) by comparative analysis of the adsorption measurements with reference data for hydrophobic and hydrophilic substrates and (2) by using the ratio of the heats of immersion in water and hydrocarbon. Hydroxylated silica gel may be used as a true hydrophilic substrate since it is covered by about 6.75 hydroxyl groups/100 A^2 (Dzhigit, Kiselev, & Muttik, 1961).

Fig. 2 shows the absolute water isotherms on the entirely hydroxylated silica gel taken from (Dzhigit et al., 1961). A comparative analysis of the initial parts of the water isotherms, which shape is determined by the polarity of the accessible surface, shows the high extent of polarity of the Palas soot surface. If the amount of water adsorbed per unit surface of silica gel at $p/p_s = 0.2$ is used as a hydrophilicity reference, then Palas soot seems to be 2.85 times less hydrophilic than the reference hydrophilic substrate but 135 times more hydrophilic than the hydrophobic reference material, graphitized soot Graphon. Table 1 contains the relative hydrophilicity at p/p_s=0.2 for fresh Palas soot (in the first adsorption cycle).

The isotherm of water adsorption on engine combustor soot (Popovitcheva et al., 2000) is also plotted in Fig. 2 and the relative hydrophilicity of this substrate is presented in Table 1. It is interesting to note that the relative hydrophilicity of Palas soot determined on the initial part of isotherm is not far from that of combustor soot but at $p/p_s \geqslant 0.3$ the isotherm of combustor soot rises steeply due to water adsorption in the micropores.

Moreover, it is generally accepted that the ratio of the surface areas determined for water and nitrogen adsorption can be utilized as a quantitative measure of the surface hydrophilicity (Naono & Hakuman, 1991). Ratios of S_{H20}/S_{N2} for soots under investigation and for reference substrates are also presented in Table 1. For Palas soot this ratio is $\frac{1}{10}$ indicating that 10% of the soot surface contains adsorption sites for water. FTIR spectroscopy studies of spark discharge soot showed oxygenated functionalities, such as –C–O, aromatic –C═O and carboxylic –C═O groups (Kirchner et al., 2000). Most likely water molecules are attached to them by hydrogen bonds since the heat of water adsorption on the dry soot surface is $Q_a \cong 17$ kJ/mol.

Hydrophilic heterogeneities like the active sites on hydrophobic surfaces can produce beneficial effects regarding the ice nucleation potential of particles such as silver iodide which are widely used

Table 1
Specific surface area, relative hygrophilicity at $p/p_s = 0.2$, ratio S_{H20}/S_{N2}, heats of immersion in water and benzene

Substrate	Surface area (m^2/g)	Relative hydrophilicity	S_{H20}/S_{N2}	$\Delta_i H_b$ (mJ/m^2) benzene	$\Delta_i H_w$ (mJ/m^2) water	$\Delta_i H_w/\Delta_i H_b$
Silicagel	330 (353)[a]	1	1/2.6	220[b]	210[b]	0.95
Palas soot	310 (640)	0.35	1/10	188	151	0.8
Combustor soot	48	0.6	1/3			
Graphon soot	83 (97)	0.0037	1/1500	114[b]	32[b]	0.28

[a]Values in the parentheses in the second row indicate the BET surface area which was determined before the measurements of heat of immersion.
[b]Zettlemoyer and Naraian, 1967

for artificial "seeding" of the clouds (Zettlemoyer & McCafferty, 1973). One comes to recognize that silver iodide is regarded hydrophobic in classical colloid chemistry but hydrophilic in cloud physics. It was hypothesized by Zettlemoyer, Tcheurekdjian, and Chessick (1961) that the AgI surface possess hydrophilic sites. On these sites the water molecules first adsorb in clusters to eventually form ice embryos after they have grown past the critical radius at the ambient temperature. A ratio of 1:3 or 1:4 of the BET surface areas for water to nitrogen was proposed as an important criterion of the ice-nucleating ability. Applying Zetllemoyer's criteria (Zettlemoyer et al., 1961) combustor soot appears to be a more efficient ice nuclei than Palas soot. Finally, to classify the hygroscopic properties of Palas soot we can use immersion calorimetry which is a useful technique to provide information about the surface wetting. According to the fundamentals of colloid chemistry a surface may be classified as hydrophilic if water wets the surface better then hydrocarbons (Shukin, Perzov, & Amelina, 2001). The heats of immersion in water, $\Delta_i H_w$ and in benzene, $\Delta_i H_b$, are qualitative characteristics of the wetting and surface chemistry. According to Rebinder's criterion the ratio $\Delta_i H_w/\Delta_i H_b$ can be a measure of hydrophilicity. Table 1 contains the values of $\Delta_i H_w$ and $\Delta_i H_b$ and the ratio of $\Delta_i H_w/\Delta_i H_b$ for Palas soot together with the respective data for the reference hydrophobic and hydrophilic substrates. It turns out that Palas soot compares more closely to the hydrophilic silica gel. It should be remembered that the heats of immersion were measured after the complete series of adsorption experiments. Therefore, the Palas soot data given in Table 1 only provide a lower limit for the hydrophilicity of this material, since it was more hydrophilic before the occurrence of structure transformation and swelling under water vapor exposure.

4. Conclusions

The adsorption and energetic properties of spark discharge soot proposed for atmospheric studies were investigated by means of gravimetry and calorimetry. Analysis of the behavior of spark

discharge soot under water exposure has shown that it exhibits a number of the specific features which do not allow us to classify this soot simply as hydrophobic or hydrophilic. According to the adsorption measurements, Palas soot compares more closely to the reference hydrophilic substrate silica gel. At low relative pressures, $p/p_S \cong 0.1$, one-tenth of the soot surface is covered by water molecules attached to the primary adsorption sites, probably related with carboxylic groups. Initially, water clusters made up of three molecules are formed, followed by capillary condensation in the interparticle mesopores at $p/p_S > 0.6$. From calorimetric data the spark discharge soot has a low-energy surface, the heat of adsorption being close to one hydrogen bond equivalent.

Emission of such soot particle agglomerates into the atmosphere will be followed by modifications of their microstructure, surface area and porosity as a result of numerical humidity fluctuations in the atmosphere. That will change their hygroscopic properties until approaching a stable state.

The question if spark discharge soot is a useful surrogate for atmospheric studies remains open since the data about the hydroscopic properties of original aircraft—generated soot are scarce until now. Some information about the growth of the monodispersed jet exhaust particles and the supersaturations needed for condensation of the particles from the jet fuel burner may be found in (Hagen, Trueblood, & Whitefield, 1992; Whitefield, Trueblood, & Hagen, 1993). But the situation is complicated because an unambiguous evidence that soot exhaust particles are directly involved in the ice formation is difficult to obtain from in situ measurements in the aircraft plume. This is why the presented data provide valuable information about the hydroscopic properties of one of the possible atmospheric soot surrogates.

Acknowledgements

Financial support from INTAS program, contract 00-0460 is gratefully acknowledged. We are grateful to Prof. U. Schurath's group from the Institute of Meteorology and Climate Research (IMK), Forschungszentrum Karlsruhe, for spark discharge soot collection. O.B. Popovitcheva acknowledges NASA for financially supporting her expert visit to IMK during the AIDA soot characterization campaign, October 1999. The authors thank Dr. K.-H. Naumann, Dr. H. Saathoff, and Dr. E. Weingartner for their interest and comments, and Dr. E. Katz for corrections and improvements.

References

Bailey, A., Cadenhead, D. A., Davies, D. H., Everett, D. H., & Miles, A. J. (1971). Low-pressure hysteresis in the adsorption of organics vapours by porous carbons. *Journal of the Transactions of the Faraday Society*, *67*, 231–243.

Blake, D. F., & Kato, K. (1995). Latitude distribution of black carbon soot in the upper troposphere and lower stratosphere. *Journal of Geophysical Research*, *100*, 7195–7202.

Bomchil, G., Harris, N., Leslie, M., Tabony, J., & White, J. (1979). Structure and dynamics of ammonia adsorbed on graphitized carbon black. *Journal of the Chemical Society-Faraday Transactions*, *75*(1), 1535–1541.

Brunauer, C. (1945). *Adsorption of gases and vapors*, Vol. 1. Princeton: Bureau of Plant Industry, US Department of Agriculture.

Calvet, E., & Prat, H. (1958). *Pecents progress en microcalorimetrie.* Paris.

Chughtai, A. R., Brooks, M. E., & Smith, D. M. (1996). Hydration of black carbon. *Journal of Geophysical Research*, *101*(D14), 19505–19514.

Coughlin, R. W., Elbirli, B., & Vergara-Edwadrs, L. (1982). Interparticle force conferred by capillary—condensed liquid at contact points. *Journal of Colloid and Interface Science*, *87*, 18–30.

Derkaui, A., Kiselev, A. V., & Kuznetsov, B. V. (1985). Calorimetrical measurements of heats of vapour adsorption on graphitized thermal carbon black. *Journal of the Chemical Society-Faraday Transactions*, *1*, 1685–1692.

Dubinin, M. M. (1965). Modern state of micropore filling theory for gas adsorption on carbonaceous adsorbents. *Russian Journal of Physical Chemistry*, *39*, 1305–1317.

Dubinin, M. M. (1980). Water vapor adsorption and the microporous structures of carbonaceous adsorbents. *Carbon*, *18*, 355–364.

Dubinin, M. M., & Stoeckli, H. F. (1980). Homogeneous and heterogeneous micropore structures in carbonaceous adsorbents. *Journal of Colloid and Interface Science*, *75*, 34–42.

Dzhigit, O. M., Kiselev, A. V., & Muttik, G. G. (1961). Heat of adsorption of water vapor on silica gel with hydrated and dehydrated surface. *Colloid Journal*, *23*, 553–561.

Gleitsmann, G., & Zellner, R. (1998). A modeling study of the formation of cloud condensation nuclei in the jet regime of aircraft plumes. *Journal of Geophysical Research*, *103*, 19543–19555.

Gregg, S. J., & Sing, K. S. W. (1982). *Adsorption, surface area and porosity* (2nd ed.). New York: Academic Press.

Hagen, D. E., Trueblood, M. B., & Whitefield, P. D. (1992). A field sampling of the jet exhaust aerosols. *Particle Science and Technology*, *10*, 53–63.

Helsper, C., Mölter, W., Löffler, F., Wadenpohl, C., Kaufmann, S., & Wenninger, G. (1993). Investigation of a new aerosol generator for the production of carbon aggregate particles. *Atmospheric Environment*, *27A*, 1271–1275.

Isirikyan, A. A., Kiselev, A. V., & Muttick, G. G. (1957). Convenient precision methods for measuring adsorption and differential heats of adsorption of vapors. In E. Schullman (Ed.), *Proceedings of the second international congress of surface activity*, London, Vol. 2 (pp. 214).

Kalberer, M., Ammann, M., Arens, F., Gaggeler, H. W., & Baltensperger, U. (1999a). Heterogeneous formation of nitrous acid (HONO) on soot aerosol particles. *Journal of Geophysical Research*, *104*, 13825–13840.

Kalberer, M., Ammann, M., Gäggeler, H. W., & Baltensperger, U. (1999b). Adsorption of NO_2 on carbon aerosol particles in the low ppb range. *Atmospheric Environment*, *33*, 2815–2822.

Kamm, S., Möhler, O., Naumann, K. -H., Saathoff, H., & Schurath, U. (1999). The heterogeneous reaction of ozone with soot aerosol. *Atmospheric Environment*, *33*, 4651–4661.

Karcher, B., Peter, Th., Biermann, U. M., & Schumann, U. (1996). The initial composition of jet condensation trails. *Journal of Atmospheric Science*, *53*, 3066–3082.

Karnaukhov, A. P., Fenelov, V. B., & Gavrilov, V. Yu. (1989). Study of the effect of surface chemistry and adsorbent texture on adsorption isotherms by comparative method. *Pure and Applied Chemistry*, *61*, 1913–1920.

Kirchner, U., Scheer, V., & Vogt, R. (2000). FTIR spectroscopic investigation of the mechanism and kinetics of the heterogeneous reactions of NO_2 and HNO_3 with soot. *Journal of Physical Chemistry*, *104*, 8908–8915.

Kiselev, A. V., & Jasin, Ja. I. (1985). *Gas und flussigkeits adsorptionschromatographie*. Berlin: VEB Deutscter Verlag der Wissenschafter.

Kiselev, A. V., & Kovaleva, N. V. (1959). Influence of thermal treatment of different soots on vapor adsorption. *Bulletin of the Academy of Science of USSR, Division of Chemical Science*, *N6*, 989–998.

Kiselev, A. V., Kovaleva, N. V., & Korolev, A. Ya. (1961). Adsorption properties of oxidized soots. *Colloid Journal*, *XXIII*, 582–591.

Kotzick, R., Panne, U., & Niessner, R. (1997). Changes in condensation properties of ultrafine carbon particles subjected to oxidation by ozone. *Journal of Aerosol Science*, *28*, 725–735.

Kuznetsov, B. V., Moreva, A. A., & Rakhmanova, T. A. (2000). Comparison of gravimetrical, volumetrical and gas chromotografical methods of adsorption measurements. *Russian Journal of Physical Chemistry*, *74*, 1507–1611.

Mikhailov, E. F., Vlasenko, S. S., Kiselev, A. A., & Ryshkevich, I. I. (1998). Restructuring factors of soot particles. *Izvestiya Atmospheric and Ocean Physics*, *34*, 307–317.

Naono, H., & Hakuman, M. (1991). Analysis of adsorption isotherms of water vapor for nonporous and porous adsorbents. *Journal of Colloid and Interface Science*, *145*, 405–412.

Nink, A., Saathoff, H., Schnaiter, M., & Möhler, O. (2001). *Laboratory investigation of the impact of aircraft particulate emissions on cirrus cloud formation.* Air pollution research report 74 "Aviation, aerosols, contrails and cirrus clouds", EC, pp. 149–153.

Poloiakova, I. G., Tarasevich, Yu. I., & Poloiakov, V. E. (1994). Studies of water vapor–carbon fiber interaction by adsorption—calorimetry techniques. *Theoretical and Experimental Chemistry*, *30*, 69–72.

Popovitcheva, O. B., Persiantseva, N. M., Trukhin, M. E., Rulev, G. B., Shonija, N. K., Buriko, Yu. Ya., Starik, A. M., Demitdjian, B., Ferry, D., & Suzanne, J. (2000). Experimental characterization of aircraft combustor soot: Microstructure, surface area, porosity and water adsorption. *Physical Chemistry and Chemical Physics*, *2*, 4421–4426.

Popovitcheva, O. B., Trukhin, M. E., Persiantseva, N. M., & Shonija, N. K. (2001). Water adsorption on aircraft-combustor soot under young plume conditions. *Atmospheric Environment*, *35*, 1673–1677.

Schwyn, S., Garwin, E., & Schmidt-Ott, A. (1988). Aerosol generation by sparc discharge. *Journal of Aerosol Science*, *19*, 639–642.

Shukin, E. D., Perzov, A. V., & Amelina, E. A. (2001). *Colloid chemistry*. Amsterdam: Elsevier Science BV.

Stoeckli, F., Perret, A., & Mena, P. (1980). Change in the microporous carbons by large moleculars. *Carbon*, *18*, 443–445.

Vartapetian, R. Sh., & Voloshchuk, A. M. (1995). Mechanism of water molecules adsorption on carbonaceous adsorbents. *Russian Chemical Reviews*, *64*, 985–1101.

Vartapetian, R. Sh., Voloshchuk, A. M., Isirikyan, A. A., & Poljakov, N. S. (1993). Energetics water cluster formation on hydrophobic surface at water vapors saturation. *Colloid Journal*, *55*, 191–192.

Weingartner, E., Burtscher, H., & Baltensperger, U. (1997). Hygroscopic properties of carbon and diesel soot particles. *Atmospheric Environment*, *31*, 2311–2327.

Wentzel, M., Gorzawski, H., Naumann, K. -H., Saathoff, H., & Weindruch, S. (2003). Transmission electron microscopical and aerosol dynamical characterization of soot and ammonium sulfate/soot mixtures. *Journal of Aerosol Science*, *34*, 1347–1370.

Whitefield, P., Trueblood, M. B., & Hagen, D. E. (1993). Size and hydration characteristics of laboratory simulated jet engine combustion aerosols. *Particle Science and Technology*, *11*, 25–36.

Young, G. J., Chessick, J. J., Healey, F. H., & Zettlemoyer, A. C. (1954). Thermodynamics of the adsorption of water on graphon from heats of immersion and adsorption data. *Journal of Physical Chemistry*, *58*, 313–315.

Zettlemoyer, A. C., & McCafferty, E. (1973). Water on oxide surfaces. *Croatica Chemica Acta*, *45*, 173–186.

Zettlemoyer, A., & Naraian, K. (1967). Heats of immersion and interface surface of vapor–solid. In E. A. Flood (Ed.), *The solid–gas interface*, Vol. 2 (pp. 129–149). New York: Marcel Dekker.

Zettlemoyer, A. C., Tcheurekdjian, N., & Chessick, J. J. (1961). Surface properties of silver iodide. *Nature*, *N18* (4803), 653.